Methanol Synthesis

Deutsche Ausgabe: DOI: 10.1002/ange.201603368
Internationale Ausgabe: DOI: 10.1002/anie.201603368

Bridging the Time Gap: A Copper/Zinc Oxide/Aluminum Oxide Catalyst for Methanol Synthesis Studied under Industrially Relevant Conditions and Time Scales

Thomas Lunkenbein[+], Frank Girgsdies, Timur Kandemir, Nygil Thomas, Malte Behrens, Robert Schlögl, and Elias Frei[+]**

Abstract: *Long-term stability of catalysts is an important factor in the chemical industry. This factor is often underestimated in academic testing methods, which may lead to a time gap in the field of catalytic research. The deactivation behavior of an industrially relevant Cu/ZnO/Al_2O_3 catalyst for the synthesis of methanol is reported over a period of 148 days time-on-stream (TOS). The process was investigated by a combination of quasi in situ and ex situ analysis techniques. The results show that ZnO is the most dynamic species in the catalyst, whereas only slight changes can be observed in the Cu nanoparticles. Thus, the deactivation of this catalyst is driven by the changes in the ZnO moieties. Our findings indicate that methanol synthesis is an interfacially mediated process between Cu and ZnO.*

Methanol, one of the most important industrial chemicals, is produced from syngas (CO, CO_2, and H_2) over ternary Cu/ZnO/Al_2O_3 catalyst at high pressure (50–80 bar) and elevated temperatures (240–280 °C). As a consequence of its high energy density (15.8 MJ/L), methanol is considered a prospective key substance for chemical energy and hydrogen storage.[1] However, its applicability as a renewable fuel is still limited by the low efficiency, and cost intensive nature of the synthetic process. Improving and understanding this catalytic process is of great interest but remains rather complex. Since the advent of increasingly sophisticated new analytical tools, the amount of generated knowledge in the field of methanol synthesis has increased enormously. The majority of the produced data can be grouped into the following three different strategies: 1) mechanistic insights into the working catalysts with a pronounced theoretical support, often on model systems;[2] 2) empirical development of new and more efficient methanol catalysts;[3] and 3) increasing the catalytic stability of the industrially relevant catalysts.[4] To date, more than 95 % of the current academic research is based on the first two approaches. Although the working mechanisms of industrial methanol catalyst have been investigated extensively, its actual active phase is still under debate and candidates range from pure Cu surfaces[5] over an active $Cu^{\delta+}$-*O*-Zn[6] interface and/or a synergy[7] between Cu-ZnO, to an active CuZn surface alloy.[8] This catalytic odyssey may be caused by a diversity of different materials and synthesis/testing methods applied, which often do not mirror industrially relevant conditions. The diversity of results further underlines the difficulties in investigating this complex catalytic material, and shows the importance of transmitting the applied industrial process parameters in the academic world.

The lifetime of an industrially applied catalyst for the synthesis of methanol is an important factor. As opposed to industrial methods, standard academic test procedures reveal experiments of only a few hours TOS, or are conducted using an accelerated aging approach.[9] This suggests the presence of a time gap between industrially relevant and academic testing conditions. Thus, conclusions considering the long-term performance may be based on extrapolated data and/or may be speculative.

However, the development of a research concept tackling long-term stability requires knowledge of the mechanism of deactivation. Herein, we report on a study of the catalytic activity of an industrially relevant Cu/ZnO/Al_2O_3 catalyst over a period of 148 days TOS under relevant conditions (60 bar, 230 °C, syngas (8 CO_2/6 CO/59 H_2/27 inert)). Several grams of the industrial catalyst were retrieved from the catalyst bed after 0, 15, 30, 50, 102, and 148 days TOS. All batches were recovered and transferred without exposure to ambient air. Subsequently, the samples were analyzed by a series of independent integral and differential methods. These ranged from quasi in situ neutron diffraction (ND) over ex situ techniques such as high resolution transmission

[*] Dr. T. Lunkenbein,[+] Dr. F. Girgsdies, Prof. Dr. R. Schlögl, Dr. E. Frei[+]
Department of Inorganic Chemistry
Fritz-Haber-Institut der Max-Planck Gesellschaft
Faradayweg 4–6, 14195 Berlin (Germany)
E-mail: lunkenbein@fhi-berlin.mpg.de
efrei@fhi-berlin.mpg.de

Dr. T. Kandemir
Hamburg University of Technology
Institute of Chemical Reaction Engineering
Eißendorfstr. 38, 21073 Hamburg (Germany)

Dr. N. Thomas
Department of Chemistry, Nirmalagiri College
Kannur, Kerala (India)

Prof. Dr. M. Behrens
University of Duisburg-Essen; Faculty of Chemistry and CENIDE
Universitätsstrasse 7, 45141 Essen (Germany)

Prof. Dr. R. Schlögl
Department of Heterogeneous Reactions
Max-Planck-Institute for Chemical Energy Conversion
Stiftstrasse 34–36, 45470 Mülheim an der Ruhr (Germany)

[+] These authors contributed equally to this work.

Supporting information for this article, including details regarding the synthesis of Cu/ZnO/Al_2O_3, catalytic pre-treatment and tests, and the applied characterization tools, can be found under: http://dx.doi.org/10.1002/anie.201603368.

electron microscopy (HRTEM), to surface sensitive measurements such as specific surface area (BET-SA), N_2O reactive frontal chromatography (RFC), and H_2 transient adsorption (TA), which address all important components in this ternary catalytic system. In general, quasi in situ ND describes the investigation of the catalyst by ND; samples were exposed repeatedly to the catalytic environment outside the diffractometer and transferred without exposure to ambient air.[10] This technique can be considered as an alternative tool for long-term studies, in particular, when irreversible or equilibrated structural phenomena are investigated.

ND is also a suitable technique to characterize heterogeneous catalysts in situ under working conditions, and to study their structural transformation.[11] The ND data provides important integral information, such as phase compositions and domain sizes of the catalyst material after different TOS durations. The parameters were extracted by full-pattern analysis with the Rietveld method using TOPAS 5[12] over a wide 2θ range. Figure 1 illustrates the ND pattern excerpts of Zn-containing phases and Cu, obtained after 0 days (Figure 1 a,b) and 148 days (Figure 1 c,d) TOS. The 0 days TOS sample was measured after reaching steady conditions under the respective pressure and temperature. For all measurements, the theoretical fit agrees reasonably well with the experimental and shows only minor deviations. Full ND patterns pertaining to Figure 1, and of all batches, are provided in the Supporting Information.

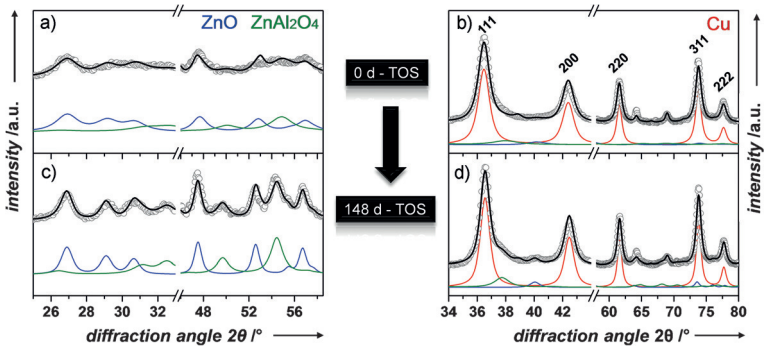

Figure 1. Quasi in situ ND measurements. Excerpts of the ND patterns (grey circles) after the a,b) first contact with the reaction feed (0 days) and c,d) 148 days TOS. The total fit curve (black), and the relevant phases Cu (red), ZnO (blue), and Zn,Al-spinel (green) are shown (the complete ND pattern is shown in the Supporting Information, Figures S1 and S2).

Only reflections that correspond to metallic Cu, ZnO, and $ZnAl_2O_4$ (Zn,Al-spinel) are observed. For the 0 days TOS measurements, weak reflections correspond to nanocrystalline ZnO and Zn,Al-spinel (Figure 1 a). Metallic Cu^0 is the most dominant phase and can be assigned to the most pronounced reflections (Figure 1 b). As opposed to the ND pattern of the 0 days TOS batch, the ND pattern of catalyst removed after 148 days TOS (Figure 1 c,d) consists of sharper reflections (see the evolution of domain sizes in Figure 2). However, only minute changes in the sharpness of the ND reflections corresponding to Cu^0 can be found (Figure 1 d). As highlighted in Figure 1 c, the situation is different for the Zn-containing phases (ZnO and Zn,Al-spinel). After the long-term experiment both oxide phases are significantly more crystalline compared to the initial sample. It should be noted, the fit model used interprets the sample contribution to the ND peak broadening exclusively in terms of the size effect. Although defects, such as strain or stacking faults, may also contribute to the ND pattern to some degree,[11a] a reasonable deconvolution of these factors cannot be obtained because of the complexity of the multiphase pattern.

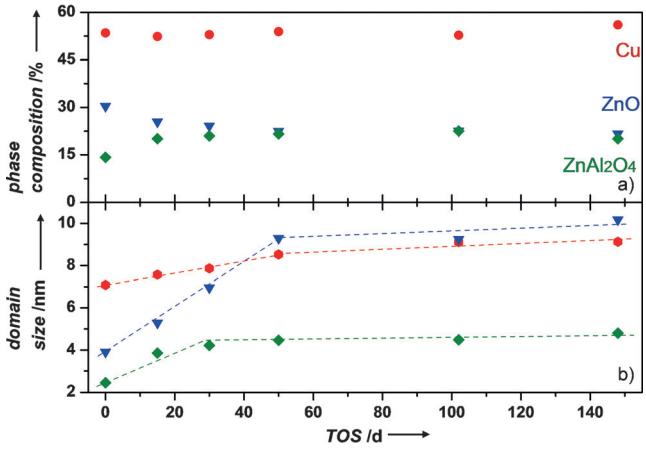

Figure 2. Quantitative analysis of the ND data. a) Phase composition of Cu, ZnO, and Zn,Al-spinel of the catalysts over different TOS durations. The data were obtained by Rietveld refinement of the ND patterns. b) Volume weighted mean domain sizes (L_{vol}-IB) of the corresponding phases, calculated from the width of the reflections. Key: Cu NPs (red), ZnO (blue), Zn,Al-spinel (green).

As revealed by the quantitative evaluation of the ND patterns (Figure 2) the Cu content within the crystalline phases of the industrially relevant catalyst does not change significantly and remains almost constant at 50 % for all TOS (Figure 2 a). A more severe change is displayed in the content of ZnO and Zn,Al-spinel (Figure 2 a). In the first 50 days TOS the catalyst is modified by an enrichment of the crystalline Zn,Al-spinel phase (14 to 21 %), whereas in the same time frame the crystalline content of the ZnO phase is significantly reduced (30 to 23 %). This trend indicates that initially amorphous Al-oxide species crystallize under reaction conditions into Zn,Al-spinel upon consumption of crystalline ZnO.

Figure 2 b shows the domain sizes of Cu nanoparticles, ZnO, and Zn,Al-spinel. The coherent scattering domain sizes of the Cu nanoparticles increases slightly (7.1 ± 0.2 to 9.1 ± 0.3 nm) during the prevailing time of the catalytic reaction (Figure 2 b). The increase of the Cu crystallite size is in agreement with the observed slight sharpening of the reflections (Figure 1) and can be attributed to a weak sintering of the metal component. For the nanocrystalline Zn,Al-spinel a more pronounced increase in the domain sizes from 2.4 ± 0.5 to 4.2 ± 0.6 nm is found for the first 30 days TOS, which remains constant for longer TOS. The ZnO

nanoparticles exhibit the strongest modifications in the domain sizes in the first 50 days TOS. The coherent scattering domain is enlarged by 138% from 3.9 ± 0.7 to 9.3 ± 1.3 nm. Thus, the observed alterations in the ND pattern can be assigned to two competing processes that seem to be detrimental for the long-term stability of Cu based industrially relevant catalysts: 1) the formation and crystallization of Zn,Al-spinel and 2) the sintering of the ZnO nanocrystals. To which extent one process influences or supports the other process remains unclear, but it seems likely that the crystallization of the Zn,Al-spinel occurs after a change of the metastable ZnO phase into a phase that is stable under normal reaction conditions. The catalyst consists of 12 wt% Al^{3+}. Behrens et al. have shown that upon reductive activation, parts of the Al^{3+} (3–4 wt%) will form a solid solution with the ZnO moieties, which leads to structural and electronic promotion of the intrinsic catalytic performance.[3a] Additionally, ZnO:Al also possesses a higher sinter resistance compared to pure ZnO.[13] The excess Al^{3+} likely remains as ND amorphous γ-Al_2O_3, which is a defective spinel structure and can react with ZnO to form a dispersed Zn,Al-spinel (Figure 1) during the methanol synthesis. After 30 days TOS the γ-Al_2O_3 is consumed and the absence of direct Zn,Al-spinel contacts may prevent further sintering. In the time period from 30 to 50 days TOS, sintering and growth of the remaining ZnO nanoparticles continues. These two phenomena indicate that in an early TOS state the dissolved Al^{3+} in ZnO is also consumed and forms the spinel phase, which diminishes the sinter resistivity of ZnO. After 50 days TOS the occurrence of larger ZnO nanoparticles may decelerate sintering processes.

The mobility of the ZnO phase in the investigated industrially relevant Cu/ZnO/Al_2O_3 catalyst can be visualized by a comparative HRTEM study of batches retrieved from the catalyst bed after 0 days TOS (Figure 3a) and 148 days TOS (Figure 3b). The overview TEM image in Figure S3a (Supporting Information) shows a porous microstructure of the catalyst after 0 days TOS with well-separated particles. Moreover, we have recently reported on the occurrence of a graphitic-like ZnO_{1-x} overgrowth on top of the nanostructured Cu nanoparticles, which is formed after reductive activation.[14] After contact with syngas at high pressures the HRTEM image obtained (Figure 3a) demonstrates a partial

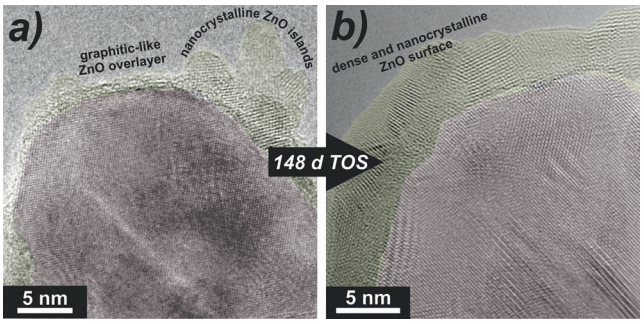

Figure 3. ZnO mobility on Cu nanoparticles after different TOS durations. TEM images of a) 0 days TOS and b) 148 days TOS. ZnO moieties (yellow), Cu NPs (red). Further images are provided in the Supporting Information, Figure S3.

conversion of this metastable ZnO_{1-x} overgrowth into separated nano-islands on top of the Cu nanoparticles. In contrast, the overview image of the sample after 148 days TOS (Supporting Information, Figure S3e) shows a densely packed microstructure, indicating agglomeration of the catalyst. The HRTEM image (Figure 3b) further reveals a dense polycrystalline ZnO layer on top of the defective Cu nanoparticles. No graphitic-like ZnO_{1-x} overgrowth was observed. Additionally, all TEM images in Figure 3 and Figure S3 (Supporting Information) suggest that the Cu nanoparticles act as supports for the ZnO moieties.

The TEM images revealed severe changes in the local surface composition of the catalyst resulting from the transformation of the Zn-containing phases, which are initially kinetically stabilized; for example, the ZnO_{1-x} overlayer and ZnO:Al phase. Moreover, the observed reflections in the detailed ND analysis after 148 d TOS (Figure 1c) arise from the stable wurtzite ZnO nanocrystals. The changes of the catalyst are induced by the reaction conditions (time (t) and pressure (p)) and the chemical potential of the gas feed. In our case the structural and surface transformation (that is, the sintering of the ZnO nanoparticles), the densification of the ZnO on the Cu surfaces, and the Zn,Al-spinel formation, are irreversible processes and evolve under the self-regulated chemical potential (see catalytic activity in Figure 4b). The self-regulating process of the chemical potential is adjusted by the partial pressure variations of the individual gaseous educts and products, which are in contact with the catalyst particles and can be derived from the changes observed in the activity data (Figure 4b). For instance, the metastable ZnO crystallites are converted into stable wurtzite ZnO and Zn,Al-spinel phases, which represent the global minimum on the energy hyperspace under these conditions.

To study the consequences of the altered surface quantitatively, a sequence of different sorption experiments was conducted (Figure 4a). From nitrogen sorption experiments, the specific BET-SA of the catalysts after different TOS durations were calculated and plotted in Figure 4a. The BET-SA decreases in the first 50 days TOS from 68 to 44 $m^2 g^{-1}$ and remains almost constant for longer TOS (44 to 39 $m^2 g^{-1}$). N_2O-RFC measurements allow the quantification of the Cu surface area and redox active sites on ZnO, which are interpreted as oxygen vacancies in ZnO_{1-x} or Zn sites of a surface alloy (Figure 4a).[15,16]

The N_2O-SA shows a strong decrease from 19 to 14.5 $m^2 g^{-1}$ within the first 50 days TOS, followed by a slight reduction of the N_2O-SA until 148 days TOS from 14.5 to 11 $m^2 g^{-1}$. Both Cu-SA and oxygen vacancies are measured, therefore a detailed interpretation of the N_2O-SA data can only be obtained if the pure Cu-SA is considered. The Cu-SA was measured by applying the H_2-TA technique (Figure 4a).[15] The difference in N_2O-SA and Cu-SA can be interpreted as a measurement for the amount of partially reduced ZnO_x sites that likely play a synergistic role in methanol synthesis over Cu-based catalysts. The Cu-SA stays almost constant (ca. 10 $m^2 g^{-1}$) in the first 50 days TOS, indicating that the loss of the N_2O-SA can mostly be assigned to a reduction of the oxygen vacancies within the ZnO_{1-x} moieties. The behavior of the sorption experiments parallels

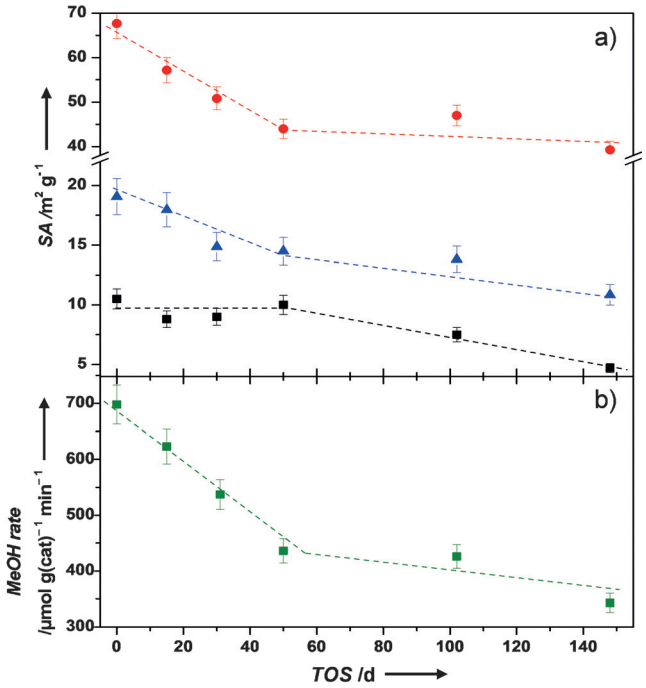

Figure 4. Surface characteristics and activity data of the catalyst for different TOS durations. a) Surface sensitive sorption measurements. Key: specific surface of the system as derived from the BET method (red), N_2O-RFC measurements resulting in Cu surface area plus redox active sites on ZnO (blue), H_2-TA data showing the actual Cu surface area (black). b) Activity data of the catalyst. All data are plotted against the TOS. The dashed lines are visual guides.

the sintering course of the ZnO domains, which also stopped after 50 days TOS.

As soon as the ZnO domains are structurally stabilized, the Cu-SA starts to decrease from 10 to 5 $m^2 g^{-1}$. According to Figure 3b and Figures S3f and S3g (Supporting Information), a dense and nanocrystalline layer of ZnO covers the Cu particles and limits the diffusion of N_2O and H_2 to the Cu surfaces. Although the ZnO coverage appears rather dense in the TEM images, a Cu surface area can be measured. This contradicting observation suggests the presence of either certain penetration pathways in the polycrystalline ZnO overlayer, or that there is indeed some free Cu surface area available. This discrepancy cannot be ruled out by the two-dimensional structural representation obtained from the TEM images. Additionally, the crystallization of the Zn-containing phases causes changes in the Cu/ZnO interface. These changes may induce a dynamic mesoscopic process (agglomeration) and can explain the slight decrease of the N_2O-SA and BET-SA after 50 versus 148 days TOS.

The influence of the above mentioned structural and surface modifications on the catalytic activity in methanol synthesis is displayed in Figure 4b. Similar to the crystallization and sintering of the ZnO nanoparticles (Figure 1), as well as to the sorption experiments (Figure 4a), the rate of methanol production strongly decreases for the first 50 days TOS. However, for further TOS only a minor change can be observed. Thus, the catalytic activity can be directly correlated to the decrease of the surface properties. The intrinsic high activity, accompanied with a metastable polymorph of ZnO, underlines the relevance of high-energy structures generating the active phases in catalysis under reaction conditions.[17] Subsequently, energetically driven alteration of the ZnO moieties, including the induction of crystallization and sintering of ZnO, causes a decrease in the catalytic activity, which can also be attributed to the loss of oxygen vacancies (as shown by the N_2O measurements in Figure 4a). As opposed to shorter TOS, where rapid sintering of ZnO and Zn,Al-spinel dominates the deactivation, after 50 days TOS "slow" sinter processes in the Zn-containing phases and Cu nanoparticles (Figure 2b) are observed. These "slow" sinter processes flatten the H_2-TA curve (and N_2O-RFC, Figure 4a), indicating that the loss in surface area is now not exclusively due to the covering of the Cu particles and the loss of interphase, but is also due to an increase of the particle sizes. Thus, for the slight decrease in activity after 50 days TOS, the sintering of the Cu nanoparticles may be considered as an additional deactivation phenomenon. Furthermore, the results suggest that the minute changes of the Cu moieties (as the main compound of the catalyst) have little impact on the performance of the catalyst within the first 50 days TOS, when the decisive deactivation occurs. The accessible Cu-SA remains almost stable for this time span, but the activity decreases enormously.

In conclusion, our findings lead to two new insights into industrially relevant $Cu/ZnO/Al_2O_3$ catalysts for methanol synthesis. 1) The early deactivation mechanism is dominated by the partial restructuring of the ZnO moieties associated with the recrystallization of the whole ZnO phase. This influences the stability of the interface between ZnO and Cu. Furthermore, the finding highlights the role of ZnO as a co-catalyst, rather than a support that prevents the Cu nanoparticles from sintering. It is therefore insufficient to describe industrially relevant methanol catalysts only with a Cu surface model. Moreover, the copper surface area obtained by N_2O-RFC measurements are often interpreted as "Cu-SA", although they also quantify additional redox active sites on reduced ZnO_{1-x}.[16] A possible scenario, in which the important role of Cu can be highlighted, is an interfacially mediated catalytic process between Cu-ZnO or $Cu^{\delta+}$-*O*-ZnO, which was already discussed in the literature as a candidate for the active phase.[6] The crystallization of ZnO moieties leads to a loss of this interface and to deactivation. This process explains the trends observed in the catalytic and surface sensitive data. Thus, the deactivation data excludes a surface alloy or unpromoted Cu as candidates for an active site. The $Cu/Cu^{\delta+}$-ZnO synergy (quantified by the difference of N_2O-SA and Cu-SA) is also strongly affected by the dynamics of the catalyst, but is still present at 148 days TOS (N_2O-SA > Cu-SA). 2) The results of this long-term deactivation study demonstrate the importance of investigating the catalyst performance for industrially relevant TOS, which gives rise to a time gap in conventional academic studies. Furthermore, the materials gap underestimates the role of ZnO as the most mobile compound in the system. Finally, the control of the dynamic nature of ZnO under the working conditions, and its promotion by Al^{3+}, seems to be the key parameter for

stabilizing the catalyst and its activity over a long TOS duration.

Acknowledgements

Maike Hashagen is acknowledged for the measurement of the BET-SA under inert conditions.

Keywords: catalyst deactivation · heterogeneous catalysis · interphase stability · methanol synthesis · quasi in situ measurements

How to cite: *Angew. Chem. Int. Ed.* **2016**, *55*, 12708–12712
Angew. Chem. **2016**, *128*, 12900–12904

[1] a) F. Asinger, *Methanol—Chemie- und Energierohstoff: die Mobilisation der Kohle*; *mit 175 Tabellen*, Akademie-Verlag, New York, **1987**; b) G. A. Olah, G. K. Surya Prakash, *Beyond Oil and Gas: The Methanol Economy*, Wiley-VCH, Weinheim, **2011**; c) R. Schlögl, *Angew. Chem. Int. Ed.* **2015**, *54*, 4436–4439; *Angew. Chem.* **2015**, *127*, 4512–4516.

[2] a) L. C. Grabow, M. Mavrikakis, *ACS Catal.* **2011**, *1*, 365–384; b) M. Behrens, F. Studt, I. Kasatkin, S. Kühl, M. Hävecker, F. Abild-Pedersen, S. Zander, F. Girgsdies, P. Kurr, B.-L. Kniep, M. Tovar, R. W. Fischer, J. K. Nørskov, R. Schlögl, *Science* **2012**, *336*, 893–897; c) F. Studt, M. Behrens, E. L. Kunkes, N. Thomas, S. Zander, A. Tarasov, J. Schumann, E. Frei, J. B. Varley, F. Abild-Pedersen, J. K. Nørskov, R. Schlögl, *ChemCatChem* **2015**, *7*, 1105–1111; d) Y. Yang, C. A. Mims, D. H. Mei, C. H. F. Peden, C. T. Campbell, *J. Catal.* **2013**, *298*, 10–17.

[3] a) M. Behrens, S. Zander, P. Kurr, N. Jacobsen, J. Senker, G. Koch, T. Ressler, R. W. Fischer, R. Schlögl, *J. Am. Chem. Soc.* **2013**, *135*, 6061–6068; b) J. Schumann, T. Lunkenbein, A. Tarasov, N. Thomas, R. Schlögl, M. Behrens, *ChemCatChem* **2014**, *6*, 2889–2897; c) E. Frei, A. Schaadt, T. Ludwig, H. Hillebrecht, I. Krossing, *ChemCatChem* **2014**, *6*, 1721–1730.

[4] a) M. B. Fichtl, D. Schlereth, N. Jacobsen, I. Kasatkin, J. Schumann, M. Behrens, R. Schlögl, O. Hinrichsen, *Appl. Catal. A* **2015**, *502*, 262–270; b) G. Prieto, J. Zečević, H. Friedrich, K. P. de Jong, P. E. de Jongh, *Nat. Mater.* **2013**, *12*, 34–39; c) S. Natesakhawat, P. R. Ohodnicki, B. H. Howard, J. W. Lekse, J. P. Baltrus, C. Matranga, *Top. Catal.* **2013**, *56*, 1752–1763; d) M. Twigg, M. Spencer, *Top. Catal.* **2003**, *22*, 191–203; e) C. H. Bartholomew, *Appl. Catal. A* **2001**, *212*, 17–60; f) H. H. Kung, *Catal. Today* **1992**, *11*, 443–453.

[5] a) J. Yoshihara, C. T. Campbell, *J. Catal.* **1996**, *161*, 776–782; b) M. Kurtz, N. Bauer, H. Wilmer, O. Hinrichsen, M. Muhler, *Chem. Eng. Technol.* **2004**, *27*, 1146–1150.

[6] K. Klier, *Adv. Catal.* **1982**, *31*, 243–313.

[7] a) J. Xiao, T. Frauenheim, *J. Phys. Chem. Lett.* **2012**, *3*, 2638–2642; b) J. Wang, S. Funk, U. Burghaus, *Catal. Lett.* **2005**, *103*, 219–223.

[8] a) Y. Choi, K. Futagami, T. Fujitani, J. Nakamura, *Appl. Catal. A* **2001**, *208*, 163–167; b) M. S. Spencer, *Top. Catal.* **1999**, *8*, 259–266.

[9] J. Agrell, M. Boutonnet, I. Melián-Cabrera, J. L. G. Fierro, *Appl. Catal.* **2003**, *253*, 201–211.

[10] S. R. K. Malladi, F. D. Tichelaar, Q. Xu, M. Y. Wu, H. Terryn, J. M. C. Mol, F. Hannour, H. W. Zandbergen, *Corros. Sci.* **2013**, *69*, 221–225.

[11] a) T. Kandemir, F. Girgsdies, T. C. Hansen, K.-D. Liss, I. Kasatkin, E. L. Kunkes, G. Wowsnick, N. Jacobsen, R. Schlögl, M. Behrens, *Angew. Chem. Int. Ed.* **2013**, *52*, 5166–5170; *Angew. Chem.* **2013**, *125*, 5271–5276; b) T. Kandemir, D. Wallacher, T. Hansen, K.-D. Liss, R. Naumann O'Alnoncourt, R. Schlögl, M. Behrens, *Nucl. Instrum. Methods Phys. Res. Sect. A* **2012**, *673*, 51–55.

[12] B. A. G., *Diffrac.Suite Topas*, version 5, Bruker AXS Inc., Madison, Wisconsin, **2015**.

[13] J. Schumann, M. Eichelbaum, T. Lunkenbein, N. Thomas, M. C. Álvarez Galván, R. Schlögl, M. Behrens, *ACS Catal.* **2015**, *5*, 3260–3270.

[14] T. Lunkenbein, J. Schumann, M. Behrens, R. Schlögl, M. G. Willinger, *Angew. Chem. Int. Ed.* **2015**, *54*, 4544–4548; *Angew. Chem.* **2015**, *127*, 4627–4631.

[15] a) S. Kuld, C. Conradsen, P. G. Moses, I. Chorkendorff, J. Sehested, *Angew. Chem. Int. Ed.* **2014**, *53*, 5941–5945; *Angew. Chem.* **2014**, *126*, 6051–6055; b) O. Hinrichsen, T. Genger, M. Muhler in *Studies in Surface Science and Catalysis*, *Vol. 130* (Eds.: F. V. M. S. M. Avelino Corma, G. F. José Luis), Elsevier, Dordrecht, **2000**, pp. 3825–3830.

[16] a) M. B. Fichtl, J. Schumann, I. Kasatkin, N. Jacobsen, M. Behrens, R. Schlögl, M. Muhler, O. Hinrichsen, *Angew. Chem. Int. Ed.* **2014**, *53*, 7043–7047; *Angew. Chem.* **2014**, *126*, 7163–7167; b) K. C. Waugh, *Catal. Today* **1992**, *15*, 51–75; c) G. C. Chinchen, K. C. Waugh, D. A. Whan, *Appl. Catal.* **1986**, *25*, 101–107.

[17] R. Schlögl, *Angew. Chem. Int. Ed.* **2015**, *54*, 3465–3520; *Angew. Chem.* **2015**, *127*, 3531–3589.

Received: April 6, 2016
Revised: July 21, 2016
Published online: September 8, 2016

